

# Preparation of Fluorine-Doped, Carbon-Encapsulated Hollow $\text{Fe}_3\text{O}_4$ Spheres as Efficient Anode Material for Li-ion Battery

Hongbo Geng,<sup>1,2</sup> Qun Zhou,<sup>1</sup> Yue Pan,<sup>1</sup> Hongwei Gu,<sup>1\*</sup> Junwei Zheng<sup>2\*</sup>

<sup>1</sup>Key Laboratory of Organic Synthesis of Jiangsu Province, College of Chemical, Chemical Engineering and Materials Science, Soochow University, Suzhou, China, 215123; <sup>2</sup>Institute of Chemical Power Sources, Soochow University, Suzhou, China, 215123;

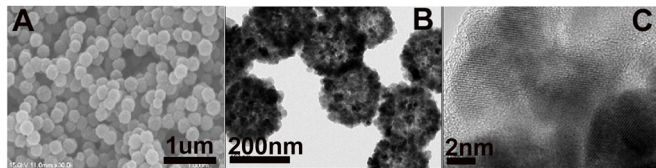


Figure S1. SEM image of the  $h\text{-}\text{Fe}_3\text{O}_4@\text{C}$  (A). TEM image of the  $h\text{-}\text{Fe}_3\text{O}_4@\text{C}$  (B). HRTEM image of the  $h\text{-}\text{Fe}_3\text{O}_4@\text{C}$  (C)

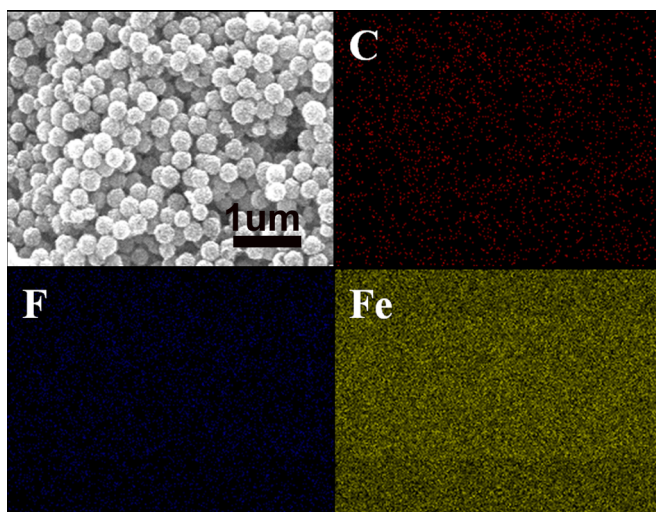


Figure S2. The energy-dispersive X-ray spectroscopy (EDX) elemental mapping of C, F and Fe in the  $h\text{-}\text{Fe}_3\text{O}_4@\text{C}/\text{F}$  composite

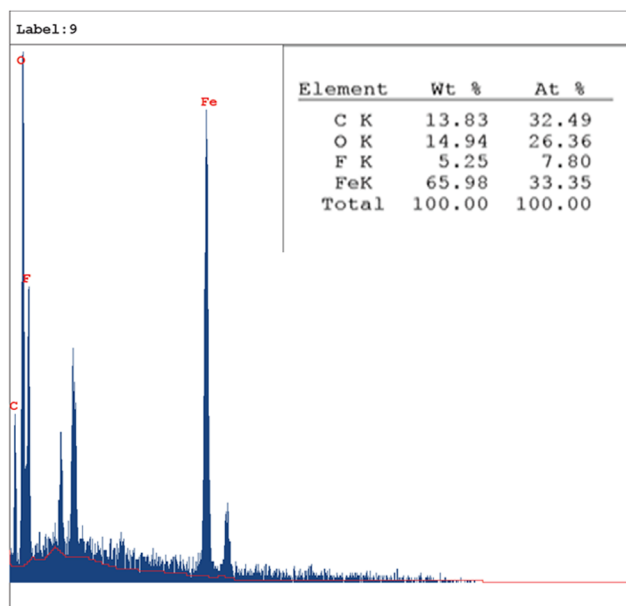


Figure S3. The energy-dispersive X-ray spectroscopy (EDX) spectrum of the  $h\text{-Fe}_3\text{O}_4@\text{C/F}$  composite

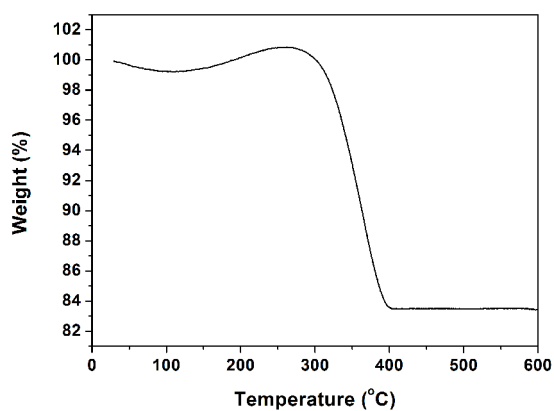


Figure S4. TGA of the  $h\text{-Fe}_3\text{O}_4@\text{C}$  composite

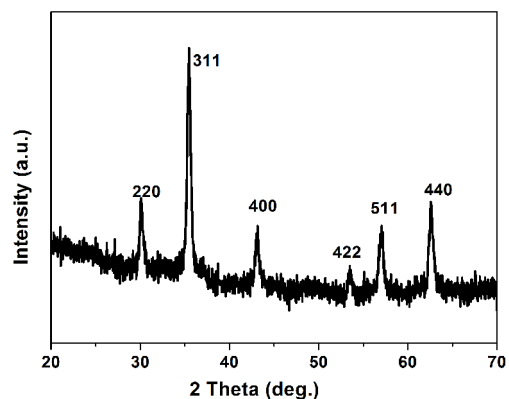


Figure S5. XRD of the  $h\text{-Fe}_3\text{O}_4@\text{C}$  composite

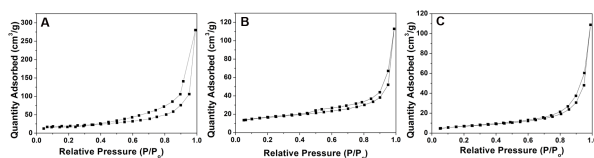


Figure S6. Nitrogen adsorption-desorption isotherm of (A)  $h\text{-Fe}_3\text{O}_4$ , (B)  $h\text{-Fe}_3\text{O}_4@\text{C}/\text{F}$  and (C)  $h\text{-Fe}_3\text{O}_4@\text{C}$ .

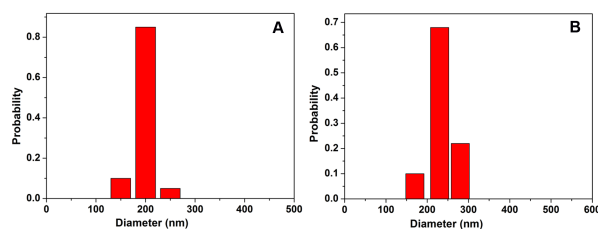


Figure S7. The diameter distributions of the (A)  $h\text{-Fe}_3\text{O}_4$  and (B)  $h\text{-Fe}_3\text{O}_4@\text{C}/\text{F}$ .

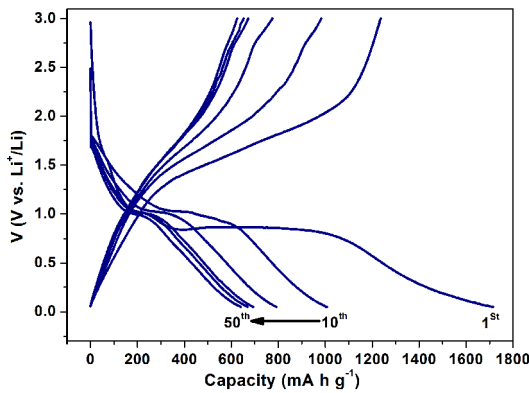


Figure S8. The charge-discharge voltage profiles of the  $h\text{-Fe}_3\text{O}_4@\text{C}$  composite

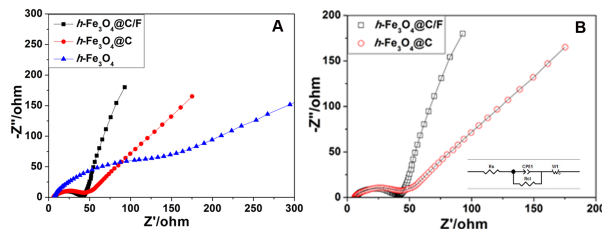


Figure S9. The impedance measures of the  $h\text{-Fe}_3\text{O}_4$ ,  $h\text{-Fe}_3\text{O}_4@\text{C}$  and  $h\text{-Fe}_3\text{O}_4@\text{C}/\text{F}$ .